LUND UNIVERSITY

Acute pyelonephritis and renal scarring are caused by dysfunctional innate immunity in mCxcr2 heterozygous mice.

Svensson, Majlis; Yadav, Manisha; Holmqvist, Bo; Lutay, Nataliya; Svanborg, Catharina; Godaly, Gabriela

Published in:
Kidney International

DOI:
10.1038/ki.2011.257

2011

Link to publication

Citation for published version (APA):
Svensson, M., Yadav, M., Holmqvist, B., Lutay, N., Svanborg, C., & Godaly, G. (2011). Acute pyelonephritis and renal scarring are caused by dysfunctional innate immunity in mCxcr2 heterozygous mice. *Kidney International*, *80*(10), 1064-1072. https://doi.org/10.1038/ki.2011.257

Total number of authors:
6

General rights
Unless other specific re-use rights are stated the following general rights apply:
Copyright and moral rights for the publications made accessible in the public portal are retained by the authors and/or other copyright owners and it is a condition of accessing publications that users recognise and abide by the legal requirements associated with these rights.
• Users may download and print one copy of any publication from the public portal for the purpose of private study or research.
• You may not further distribute the material or use it for any profit-making activity or commercial gain
• You may freely distribute the URL identifying the publication in the public portal

Read more about Creative commons licenses: https://creativecommons.org/licenses/

Take down policy
If you believe that this document breaches copyright please contact us providing details, and we will remove access to the work immediately and investigate your claim.

LUND UNIVERSITY

PO Box 117
221 00 Lund
+46 46-222 00 00

Acute pyelonephritis and renal scarring are caused by dysfunctional innate immunity in *mCxcr2* heterozygous mice

Majlis Svensson[1], PhD, Manisha Yadav[1,2], PhD, Bo Holmqvist[1], PhD, Nataliya Lutay[1], PhD, Catharina Svanborg[1], MD, PhD, Professor and Gabriela Godaly[1], PhD

[1]Department of Microbiology, Immunology and Glycobiology, Institute of Laboratory Medicine, Lund University, Lund, Sweden, [2]Dr B.R. Ambedkar Centre for Biomedical Research, University of Delhi, Delhi, India

Running headline: Dysfunctional immunity in *mCxcr2*$^{+/-}$ mice.

Corresponding author:

Prof. Catharina Svanborg

Department of Microbiology, Immunology and Glycobiology

BMC, C12, Lund University

SE-223 62 Lund. Sweden

Telephone: +46 46 - 222 70 44

Fax: +46 46 - 13 74 68

E mail: Catharina.Svanborg@med.lu.se

ABSTRACT

The CXCR1 receptor and chemokine CXCL8 (IL-8) support neutrophil-dependent clearance of uropathogenic Escherichia coli from the urinary tract. CXCR1 is reduced in children prone to pyelonephritis, and heterozygous hCXCR1 polymorphisms are more common in this patient group than in healthy individuals, strongly suggesting a disease association. Since murine CXCR2 (mCXCR2) is functionally similar to human CXCR1, we determined effects of gene heterozygosity on the susceptibility to urinary tract infection by infecting heterozygous (*mCxcr2*$^{+/-}$) mice with uropathogenic *Escherichia coli*. Clearance of infection and tissue damage were assessed as a function of innate immunity, compared to *mCxcr2*$^{-/-}$ and *mCxcr2*$^{+/+}$ mice. Acute sepsis-associated mortality increased drastically in heterozygous compared to wild type mice and bacterial clearance was impaired. The chemokine and neutrophil responses were delayed and there was evidence of neutrophil retention and unresolved kidney inflammation one month after infection, accompanied by epithelial proliferation and sub-epithelial fibrosis. The heterozygous phenotype was thus intermediate, between the *mCxcr2*$^{-/-}$ and *mCxcr2*$^{+/+}$ mice, but the specific immune cell infiltrates that accompany chronic infection in *mCxcr2*$^{-/-}$ mice were not observed. The results indicate that a heterozygous *mCxcr2* defect impairs the innate immune response against acute pyelonephritis, increases the risk for urosepsis and prolongs the infection. The known heterozygous human *hCXCR1* polymorphisms might thus predispose patients to acute pyelonephritis and urosepsis.

Keywords: acute pyelonephritis, innate immunity, *mCXCR2*, renal scarring, UTI

INTRODUCTION

Genetic variation influences the resistance to common infections by modifying innate immune responses (1). Urinary tract infections (UTI) serve as an excellent example. Single gene deletions have drastic effects on UTI susceptibility in mice and human *TLR4*, *CXCR1* and *IRF3* polymorphisms have been identified in different UTI prone populations (2-4). Most of these polymorphisms affect transcription and protein expression rather than protein structure, and were first identified in patients with UTI (1). It has been estimated that >150 million adults are diagnosed with UTI each year, and in childhood, acute pyelonephritis (APN) causes kidney injury in 20-90% of the patients (5, 6). Unless properly treated, APN may cause renal scarring, potentially leading to hypertension and renal failure (7, 8). Understanding the genetic basis of UTI susceptibility and identifying patients prone to severe acute disease or tissue damage is therefore essential.

In 2000, we showed that a *mCxcr2* deletion caused unrestrained progression of experimental UTI in mice, as well as increased acute mortality and renal tissue destruction (2, 9). Furthermore, CXCR1 expression was reduced in pyelonephritis prone children compared to healthy controls (2), suggesting relevance of this genetic variant for human disease. In a subsequent study, we found five heterozygous CXCR1 sequence variants in APN prone children (10); three were unique to the APN prone group and two known variants were more common in APN patients than in controls. Variant 1 reduced RUNX1 and PU.1 dependent transcription while variants 2 and 3 disrupted putative transcription factor binding sites. Variant 5 was associated with reduced levels of the large CXCR1 transcript, suggesting that this mutation might create a more efficient cleavage site and thus reduce the amount of full length CXCR1 mRNA (11).

The CXCR1 receptor and the chemokine CXCL8 (IL-8) support the neutrophil-dependent clearance of uro-pathogenic *Escherichia coli* (UPEC) from the urinary tract (12, 13). CXCL8

binding to neutrophil hCXCR1 initiates a signalling cascade that governs neutrophil movement, phagocytic activity and the release of inflammatory mediators (14). Expression of hCXCR1 is also induced by infection of the single layer of proximal tubular epithelial cells, which forms the physical barrier against ascending UPEC infection (13). Murine CXCR2 (mCXCR2) is functionally most similar to hCXCR1, even though a putative mCXCR1 orthologue has been described (15-17). mCXCR2 is the cognate receptor for two structurally related ELR^+ chemokines, mCXCL1 (KC) and mCXCL2/3 (MIP-2), of which mCXCL2/3 has been linked to neutrophil recruitment and bacterial clearance in response to UTI (18, 19). *mCxcr2* mutant mice show a dramatic phenotype with tissue destruction resembling renal scarring in human pyelonephritis-prone individuals (9, 20). The receptor deficiency causes neutrophil entrapment beneath the mucosa, eventually destroying the mucosal barrier (2, 9, 20). A single gene defect that perturbs innate immunity is thus sufficient to cause acute susceptibility and chronic tissue pathology in the murine UTI model.

Our findings thus indicated that CXCR1 heterozygosity would result in reduced receptor expression and a blunted cellular response to UTI. To characterize the impact of heterozygous receptor expression *in vivo*, we analysed the effects of experimental UTI in receptor heterozygous mice. The results show that the reduced mCXCR2 expression in heterozygous $mCXCR2^{+/-}$ mice results in a delayed innate immune response, increased severity of infection, and significant tissue pathology. Our findings indicate that human *hCXCR1* heterozygosity might contribute to disease susceptibility.

RESULTS

mCxcr2 genotypes and effects on mCXCR2 expression

Prior to experimental infection, the mouse *mCxcr2* genotype was verified by polymerase chain reaction (PCR), using specific primers for the wild-type*mCxcr2* gene or the neomycin cassette. A single *mCxcr2* band was amplified from wild type (*mCxcr2*$^{+/+}$) mouse DNA and a single band corresponding to the neomycin cassette from homozygous (*mCxcr2*$^{-/-}$) mouse DNA (Figure 1A). Both bands were amplified from heterozygous mouse DNA (*mCxcr2*$^{+/-}$) as one copy of the gene was disrupted by the neomycin cassette.

The resulting difference in receptor expression of mCXCR2 on peripheral blood leukocytes was confirmed by flow cytometry after labelling with mCXCR2 antibody (Figure 1B). mCXCR2 expression was high in *mCxcr2*$^{+/+}$ mice (2.0 ± 0.5), intermediate in *mCxcr2*$^{+/-}$ mice (0.59 ± 0.4, $p<0.05$ compared to *mCxcr2*$^{+/+}$ mice and $p \leq 0.01$ compared to *mCxcr2*$^{-/-}$ mice) and absent in *mCxcr2*$^{-/-}$ mice ($p \leq 0.001$ compared to *mCxcr2*$^{+/+}$ mice).The difference in mCXCR2 expression was further quantified by RT-PCR. mCXCR2 mRNA levels normalized against GAPDH were compared in blood samples from *mCxcr2*$^{+/+}$, *mCxcr2*$^{+/-}$ and *mCxcr2*$^{-/-}$ mice. The expression was lower in the heterozygous mice ($p = 0.019$) than in *mCxcr2*$^{+/+}$ mice ($p < 0.001$) but higher than in *mCxcr2*$^{-/-}$ mice ($p < 0.001$) (Figure 1C).

Increased mortality in*mCxcr2*$^{+/-}$mice following experimental UTI

In *mCxcr2*$^{-/-}$ mice, experimental UTI is accompanied by sepsis and significant mortality. To address if heterozygosity influences sepsis and mortality, survival was compared between *mCxcr2*$^{+/+}$, *mCxcr2*$^{+/-}$ and *mCxcr2*$^{-/-}$ deficient mice after intravesical infection with the UPEC strain 1177, originally isolated from a child with acute pyelonephritis. Significant mortality

occurred during the first week after infection, as illustrated by the Kaplan-Mayer curve in Figure 2A; 2% of *mCxcr2*$^{+/+}$ mice, 40% of *mCxcr2*$^{+/-}$ mice and 60% of *mCxcr2*$^{-/-}$ mice developed lethal infections (p=0.004). Mortality was associated with systemic infection, as shown by positive *E. coli* cultures of blood samples obtained by cardiac puncture. Six hours after infection, no bacteria were found in the blood of *mCxcr2*$^{+/+}$ mice, but $5x10^4$ CFU/ml were found in the blood of *mCxcr2*$^{+/-}$ and *mCxcr2*$^{-/-}$ mice. After 24 hours, $1x10^4$ CFU/ml were found in blood of*mCxcr2*$^{+/+}$ mice and $4x10^6$ CFU/ml were found in the blood of *mCxcr2*$^{+/-}$ and *mCxcr2*$^{-/-}$ mice. The results suggest that *mCxcr2* heterozygous mice run an increased risk of developing septic, lethal UTI compared to wild-type mice.

Impaired bacterial clearance in *mCxcr2*$^{+/-}$mice

Experimental UTI is rapidly cleared in immunocompetent mice but delayed in *mCxcr2*$^{-/-}$mice. To address if heterozygosity influences bacterial clearance, cultures from kidneys and bladders were obtained at different times after infection. Following infection of *mCxcr2*$^{+/+}$ mice with 10^8 CFU/ml of UPEC strain1177, there was a rapid decline in renal bacterial counts and infection was cleared after about seven days (Figure 2B). In contrast, *mCxcr2*$^{+/-}$ mice showed a delay in bacterial elimination from the tissues ($p<0.01$ compared to *mCxcr2*$^{+/+}$ mice at day 7, 14 and 21). The kidneys remained infected for 21 days, before the infection was cleared. Furthermore, *mCxcr2*$^{+/-}$ mice showed intact overall renal architecture, without sub-epithelial or sub-capsular abscesses or papillary necrosis (Figure 2C). In contrast, *mCxcr2*$^{-/-}$ mice remained infected during the entire 42-day period and showed a dramatic loss of renal tissue integrity (Figure 2C). The results suggest that while bacterial clearance from the urinary tract is delayed by reduced mCXCR2 expression in *mCxcr2*$^{+/-}$ mice, overall tissue integrity remains intact.

Chemokine response to experimental UTI

Infection activates a rapid cytokine/chemokine response in the urinary tract mucosa. To address if heterozygosity influences chemokine expression, concentrations of the neutrophil specific mCXCL2/3 and the monocyte specific mCCL2 cytokines were quantified in urine samples, obtained at regular intervals after infection. The mCXCL2/3 response was high in *mCxcr2*$^{+/+}$ mice after 6 hours, but declined after 14 days (Figure 3A). In *mCxcr2*$^{+/-}$ mice, the mCXCL2/3 response was delayed but prolonged, reaching a maximum after 24 hours and remaining elevated for 28 days in most of the mice ($p<0.05$, Figure 3A). Infection did not trigger mCCL2 secretion in *mCxcr2*$^{+/+}$ type mice (Figure 3B), but in *mCxcr2*$^{+/-}$ mice, mCCL2 was present in urine during the entire study, even though the maximum level was reached after 24 h ($p<0.01$, Figure 3B). The results suggest that there are qualitative and quantitative differences in the chemokine response to UTI between *mCxcr2*$^{+/+}$ and *mCxcr2*$^{+/-}$ mice.

Impaired neutrophil recruitment in heterozygous mice

Neutrophils are essential effectors of the antibacterial defence in the urinary tract and deficient neutrophil clearance severely impair host resistance. To characterise neutrophil recruitment and clearance in *mCXCR2*$^{+/-}$ mice, neutrophils were first quantified in urine samples, obtained after 6 hours and 1, 7, 14, 28 and 42 days of infection (Figure 3C). In *mCxcr2*$^{+/+}$ mice, the increase in urine neutrophil numbers reached a peak at 6 hours followed by a decrease to background levels at 24 hours (Figure 3C). The *mCxcr2*$^{+/-}$ mice showed a first peak in urine neutrophil numbers at 6 hours, corresponding to the kinetics in control mice, but this peak was significantly lower ($p<0.05$). A second wave of neutrophil recruitment occurred in the *mCxcr2*$^{+/-}$ mice with a peak, seven days after infection ($p<0.01$). This peak was not detected in the *mCxcr2*$^{+/+}$ type mice.

Neutrophil infiltrates were subsequently examined in renal tissue sections obtained after 6 hours and after 7, 14, 28 and 35 days post infection (Figure 4). In *mCxcr2*$^{+/+}$ type mice, infection triggered a rapid, transient neutrophil influx (Figure 4A), but after seven days few neutrophils remained in renal tissues or in the lumen (Figure 4A). In *mCxcr2*$^{+/-}$ mice, a weak early neutrophil response was observed, but on day seven, a neutrophil infiltrate was noticed ($p<0.05$) and neutrophils were still found in aggregates that remained in the pelvic lumen from day 7 after infection (Figure 4B). The results suggest that despite reduced receptor expression, neutrophil recruitment occurs in *mCxcr2*$^{+/-}$ mice, with a delay compared to *mCxcr2*$^{+/+}$ wild type mice.

Chronic tissue damage

To examine the effects of heterozygosity on changes in renal tissue morphology in response to infection, haematoxylin-eosin-stained tissue sections were examined by high-resolution microscopy (Figure 5). *mCxcr2*$^{+/+}$ mice cleared the infection with only a minor epithelial proliferation 7 days after infection, but there was no evidence of fibrosis (Figure 5A). In *mCxcr2*$^{+/-}$ mice, sub-epithelial fibrosis was observed after 14 days with Masson's trichrome staining and epithelial hypertrophy was seen (Figure 5B). After 28 days, multiple layers of epithelial cells and sub-epithelial fibrosis were observed in the inflamed tissues of *mCxcr2*$^{+/-}$ mice (Figure 5B). In *mCxcr2*$^{-/-}$ mice tissue structure was initially normal post-infection, but after 7 days thickening of the pelvic epithelium and bacterial mass in the lumen was observed (Figure 5C). After 28 days of infection, the inflammatory cell infiltrate was abundant and the tubular structure was almost completely destroyed (Figure 5C).

A collected overview of the course of disease in *mCxcr2*$^{+/-}$ mice is presented in Figure 6.Larger neutrophil aggregates were observed in the lumen of *mCxcr2*$^{+/-}$ mice from 7 days after infection

up to 28 days after infection. Epithelial hypertrophy and sub-epithelial fibrosis were found with haematoxylin and Masson's trichrome staining of *mCxcr2*$^{+/-}$ mice (Figure 6).

The results suggest that reduced mCXCR2 expression and impaired innate immunity leads to a chronic inflammatory state in *mCxcr2*$^{+/-}$ mice.

Lack of monocyte/lymphocyte infiltration in heterozygous mice

Previous studies in *mCxcr2*$^{-/-}$ mice showed that the initial neutrophil recruitment in response to UTI is followed by a monocytic infiltrate, comprising lymphocytes, plasma cells and Russel bodies as well as macrophages and foam cells (20). In *mCxcr2*$^{-/-}$ mice, lymphocytes were abundant in the medulla, but also in the sub-epithelial space, albeit to a lesser extent. To examine if a similar cellular infiltrate might be established in *mCxcr2*$^{+/-}$ mice, kidney sections obtained at different times after infection were examined by immunohistochemistry after staining with antibodies specific for neutrophil, macrophage, dendritic and various lymphocyte markers. Interestingly, cells with a lymphocyte like morphology were observed throughout the kidneys, but specific antibodies did not stain this population (Figure S1). In 10% of the *mCxcr2*$^{+/-}$ mice, macrophages were observed in the cortex 42 days after infection (Figure S1).

DISCUSSION

We have detected significant effects of homozygous single gene deletions on UTI susceptibility in mice and associations of heterozygous polymorphisms to susceptibility in UTI prone patients (2-4). These results were unexpected, since single gene polymorphisms have not generally been considered sufficient to alter the susceptibility to complex clinical syndromes like APN and since the genetic variants were heterozygous, potentially leaving a reduction in function rather than a complete loss of function associated with most monogenetic disorders. However, while the heterozygous mutations have been shown to reduce gene expression in reporter assays, the functional importance of heterozygous variants for *in vivo* infection has not been defined. This study investigated if mCXCR2 heterozygosis is functionally relevant for UTI susceptibility. We found increased acute mortality in *mCXCR2*$^{+/-}$ mice, a delay in neutrophil recruitment and evidence of neutrophil retention and unresolved kidney inflammation, accompanied by epithelial proliferation and sub-epithelial fibrosis. However, unlike *mCxcr2*$^{-/-}$ mice, sub-capsular abscess formation was not observed in the heterozygous mice and the acute phase was not followed by severe tissue destruction. The results indicate that a single heterozygous mCXCR2 defect impairs critical aspects in the innate immune response, thus increasing the susceptibility to acute pyelonephritis.

Genetic variation affecting chemokine receptor expression has been shown to modify host resistance to infections. A genetic variant of *CCR5* (*delta*-32) was associated with low risk for HIV-infection and to slow disease progression (21-23). Recently, a haplotype of the human CXCR1 gene was shown to be protective against rapid disease progression in HIV-1 patients (24).The *mCxcr2*$^{+/-}$ mice showed an altered innate immune response to UTI, increased sepsis-associated mortality and impaired bacterial clearance. Uro-sepsis accounts for approximately 25% of all sepsis cases and may develop from community- or nosocomially acquired UTI (25).

Our early studies in mCXCR2$^{-/-}$mice provided the first evidence that genetic defects affecting innate immunity increase the susceptibility to uro-sepsis (2) and subsequently, single nucleotide polymorphisms in genes encoding tumor necrosis factor-β, interleukin-6, CD14 and TLR2 have been associated with sepsis (reviewed by Sutherland et al. (26)). In this study, we observed significant mortality during the first week after infection in mCXCR2$^{+/-}$ mice compared to control mice and mortality was accompanied by systemic infection. The mortality in the heterozygous group occurred during the first 24 hours (40%), but in contrast to the mCXCR2$^{-/-}$ mice, mortality does not increase further**.** It is possible that the window was caused by the delay in neutrophil recruitment in the heterozygous mice, making them ‘’homozygous-like’’ only during the first 24 hours.

The cellular origin of the cytokine response in the urinary tract has been extensively studied, both with regard to the producing cells, the virulence factors and the involved signalling pathways (4, 27-29). In response to infection with UPEC, epithelial cells produce high amounts of cytokines and chemokines, such as IL-6, CXCL1-3, CXCL8, and CCL2 in order to attract leukocytes to the place of infection. The first chemotactic signal emanates from uro-epithelial cells, which are efficient chemokine producers (28) (for review see (30, 31). Neutrophil recruitment is rapid, however, and recruited neutrophils take over as the major source of inflammatory mediators after 30 minutes to 2 hours and recruited inflammatory cells (27) contribute to the later waves of chemokine response. Bacteremic infections are likely to activate a number of additional cell types, as the bacteria cross the epithelial barrier, traverse the submucosa, and invade local blood vessels. Mesangial, endothelial, interstitial cells, and renal fibroblasts produce both CXC and CC chemokines (32, 33). In this study, the monocyte/lymphocyte chemoattractant mCCL2 was elevated in heterozygous mice, but not in

wild type mice. While a cellular infiltrate with lymphocyte like morphology was observed in the heterozygous mice, antibodies against mCXCR2, CD3, CD4 and CD8 failed to stain the cells, possibly indicating an unconventional phenotype (34). Evidence of apoptosis was not found, as TUNEL staining failed to identify the cellular infiltrate, suggesting that the "round cell'' morphology did not reflect cell death(35-37).Chemokine receptors are further involved in reconstruction of denudated areas after kidney injury (38). Cells surviving the initial injury dedifferentiate into mesenchymal phenotype, migrate into denudated area, where they proliferate back to epithelial phenotype to replace the lost cells (39). Further studies are needed to examine if such mechanisms may explain the cellular infiltrate.

The cause of renal tissue damage after infection remains poorly understood, but previous studies have suggested that the exaggerated neutrophil infiltrate and deficient neutrophil function in *mCxcr2*$^{-/-}$ mice may be a critical factor (9). mCXCR2/3 (formerly MIP-2) is one functional ortholog of the human neutrophil chemoattractant CXCL8 (formerly termed IL-8). Blocking of mCXCL2/3 in the murine UTI model has been shown to inhibit neutrophil migration across the epithelium into the urine (19). A balanced neutrophil recruitment into the tissues and exit across the epithelial barrier is essential to benefit from the antibacterial effector functions while removing the toxic neutrophil contents from the tissues. In heterozygous mice, neutrophil recruitment was delayed, but there was a construction of neutrophil infiltrate, suggesting one mechanism of tissue damage. The neutrophils were mainly located adjacent to the lumen, possibly providing a driving force for the epithelial hypertrophy and sub-epithelial fibrosis, suggesting that the reduced mCXCR2 function in these mice is insufficient to maintain proper tissue homeostasis in the infected state.

Innate immune mechanisms control the antibacterial defence of the urinary tract and maintain tissue homeostasis during infection. While hCXCR1 was the first identified

polymorphic innate immune response gene and the first genetic determinant to be associated with human UTI (2), our studies have since identified additional genetic determinants of UTI susceptibility (3, 4). Tlr4 promoter polymorphisms were recently shown to control the level of TLR4 expression and specific polymorphisms were associated with asymptomatic bacteriuria rather than acute pyelonephritis (3). Furthermore, interferon regulatory factor 3 (IRF3), which controls the transcription of several innate immune response genes including CXCL8 (4) and human IRF3 promoter polymorphisms with a strong acute pyelonephritis association were recently detected (4). These findings raise the possibility that future risk assessments in children with febrile UTI might include genetic markers. Further clinical studies are needed to demonstrate if heterozygous polymorphisms including hCXCR1 might help to predict risk for severe UTI.

MATERIAL AND METHODS

Bacteria

*E. coli*1177, serotype O:1K:1H:7, was isolated from a child with acute pyelonephritis (40) and was maintained in deep agar. *E. coli*1177is haemolysin negative but expresses P and type 1 fimbriae and is virulent in the UTI mouse model where it evokes a strong innate immune response (41). *E. coli*1177 was cultured on Tryptic soya agar (TSA) plates, harvested by centrifugation and re-suspended to a concentration of 10^9 CFU/ml. The bacterial concentration was confirmed by viable counts.

Mice

Mice were bred in the animal facilities at the Department of Microbiology, Immunology and Glycobiology, Lund University, Sweden. Breeding pairs of *mCxcr2*$^{+/-}$ and *mCxcr2*$^{-/-}$ (C.129S2(B6)-Il8rb^{tm1Mwm}/J) mice were purchased from Jackson Laboratories (Bar Harbour, ME). Congenic Balb/c mice were used as controls (*mCxcr2*$^{+/+}$). *mCxcr2*$^{-/-}$ mice fail to express mCXCR2, due to the insertion of a neomycin gene (42) and heterozygous mice express less of the receptor due to co-dominant inheritance. The study was approved by the Animal experiment ethics committee at the Lund district court in Sweden.

Genotyping by PCR

The *mCxcr2* genotype was confirmed by PCR on DNA extracted from ear clippings and blood samples of individual mice as described previously (2). Validated primers specific for the wild-type *mCxcr2* gene and the inserted neomycin gene were used (Figure 1A). Validated primers specific for the wild-type *mCxcr2* (5'-ggT CgT ACT gCg TAT CCT gCC TCAg-3' and 5'-Tag

CCA TgA TCT TgAgAAgTCC Atg-3') and for the inserted neomycin gene (5'-CTT gggTggAgAggC TAT TC-3' and5'-Agg TgAgATgACAggAgA TC-3') were used.

Experimental APN

The ascending murine UTI model has been described (43). Briefly, following anaesthesia, wild type, heterozygous and homozygous mice were infected by intra-vesical inoculation (10^9 CFU/ml, 100µl) through a soft polyethylene catheter (outer diameter 0.61 mm; Clay Adams, Parsippany, NY). The catheter was withdrawn, and the mice were allowed food and water ad libidum. Animals were sacrificed at the designated time intervals after infection, or when they developed symptoms of severe disease. The experiment was repeated four times with 5-7 mice in each group. After sacrifice, bacterial numbers in kidneys and bladders were determined by viable counts on tissue homogenates. The organs were separately placed in a sterile plastic bag containing 5 ml of phosphate buffered saline (PBS, 0.1M pH 7.2), and homogenized in a Stomacher 80 homogenizer (Seward Medical, UAC House, London). Homogenates were diluted in sterile PBS, 0.1 ml of each dilution was plated on TSA, and the number of colonies was scored after overnight culture at 37^{o}C. The contra-lateral kidney was placed in 4% paraformaldehyde (PFA) and stored for histological analysis. Mice with severe UTI symptoms were examined for bacteremia. Blood samples obtained by cardiac puncture were collected into heparin-coated tubes. 100 µl of blood was cultured on uriselect agar plates, whereupon different dilutions were tested for the different counts. Bacterial numbers were quantified after over-night culture at 37^{o}C.

Urine samples were obtained prior to infection and at regular times post-infection. Urine neutrophils were quantified in a haemocytometer chamber. mCXCL2/3 and mCCL2

concentrations in urine were quantified by ELISA (R&D Systems, Abingdon, UK), according to the manufacturer's instructions.

Histologic evaluation of acute and chronic infection

The fixed tissue samples were dehydrated by over night incubation in alcohol, followed by xylene, and placed in Histowax (Histolab Products, VästraFrölunda, Sweden) according to manufacturer's recommendations. The samples were embedded in paraffin, 4 to 5 μm sections were cut and placed on glass slides. Sections were deparaffinized and stained with hematoxylin-eosin. Masson'strichrome staining was used for detection of fibrosis, as described in Svensson et al. (20). Three individuals investigated samples independently.

Immunohistochemistry

Kidneys were placed in a freshly prepared solution of 4% PFA in PBS at 4^{o}C over night, rinsed in 15% followed by 25% ice-cold sucrose in PBS. The tissues were then frozen in isopentane at –40^{o}C and stored at –80^{o}C until sectioned. Cryostat sections were cut at a thickness of 10μm, thaw mounted onto poly-L-lysin coated glass slides, dried for 30–60 minutes and stored at –80^{o}C. The samples were graded by three independent observers.

For neutrophil staining, the sections were incubated with a 1:200 dilution of the anti-rat NIMP-R14 antibodies (Abcam, Cambridge, UK) and for macrophage staining, the sections were incubated with Macrophage Marker (RM0029-11H3) antibodies (1:40; Santa Cruz Biotechnology) for 2- 3 hr. Murine anti-CD3, anti-CD4 and anti-CD8 antibodies were used for lymphocyte staining with a 1:40 dilution for 2-3 hr (R&D Systems, UK) and murine anti-CD205

were used for dendritic staining (BioSite, USA). After staining, the slides were washed three times and developed with a solution of Alexa 488-conjugated goat anti-rat IgG (1:100, Molecular probes) for 60 minutes. The sections were incubated in DAPI (Invitrogen Molecular Probes, USA) for 5 minutes followed by rinsing in PBS. As a control, incubations with primary antibodies were excluded for one slide in every labelling experiment. All antibodies were diluted in PBS containing BSA (2%) and TX (0.05%). The slides were examined in an Olympus AX 60 microscope equipped with the fluorescence detection for Alexa Fluor 488 and DAPI, images were captured with an Olympid DP70 digital camera.

mRNA isolation

Blood was collected with heparinized RNAprotect® Animal Blood Tubes (Qiagen) to prevent the blood from coagulating. Total RNA was purified with RNeasy® Protect Animal Blood Kit (Qiagen) according to the manufactory instruction. Samples were stored at -80˚C until use.

RT-PCR

The RNA was converted to complimentary DNA (cDNA) by reverse transcription using SuperSctipt^{TM} III First-Strand Synthesis System for RT-PCR (Invitrogen, USA). Real time RT-PCR using QuantiTect® SYBR® Green PCR (Qiagen, USA) were preformed for measuring the amount of cDNA according to the manufactory instructions. The results were analysed in Rotor gene 2000 in which a cycle threshold valued (C_T) was estimated. Gene expression levels were calculated by the ΔCt method and normalized to house keeping gene. The murine housekeeping gene GAPDH (glyceraldehydes-3-phosphate dehydrogenase) was used as an internal standard. The mouse primers used for RT-PCR are GAPDH (QT01658692) and

mCXCR2 (QT00283696) were purchased from Qiagen. RT-PCR was used to compare and verify *mCxcr* expression in *mCxcr2*$^{+/-}$ and *mCxcr2*$^{-/-}$ mice versus*mCxcr2*$^{+/+}$ mice.

Flow cytometry

Blood samples were collected in heparinized tubes from a wild type mouse. Neutrophils were identified and gated by staining whole blood with 1:200 dilutions of the neutrophil specific anti-rat RB6-8C5 antibody (a kind gift from Dr. A. Sjöstedt, Umeå University, Sweden) for 30 minutes and secondary stained with Alexa 488-conjugated goat anti-rat IgG (Abcam, UK) for 60 minutes. Red blood cells were lysed by adding 2 ml FACS Lysing solution (BD Biosciences, UK). mCxcr2 expression was analysed by staining 100 μl of whole blood from *mCxcr2*$^{+/+}$, *mCxcr2*$^{+/-}$ and *mCxcr2*$^{-/-}$ mice with 10 μl of anti-mouse Cxcr2-phycoerythrin (R&D System, UK). 10 μl of IgG was used as a negative control. The samples were quantified by flow cytometry (FASC Calibur, BD Biosciences, UK).

Statistical analysis

The non-parametric Mann-Whitney U-test (two-tailed) and Fisher's exact test were used. The statistical program used was the In Stat version for Macintosh. Differences were considered significant for $p < 0.05$.

ACKNOWLEDGEMENTS

We thank Maria Friberg for technical assistance. The studies were supported by grants from the Swedish Medical Research Council (http://www.vr.se/), the Crafoord (http://www.crafoord.se/), Wallenberg (http://www.wallenberg.com/), Lundberg (http://web.lundbergsstiftelserna.se/),

Swedish Institute (http://www.si.se/) and Osterlund Foundations and the Royal Physiographic Society (http://www.fysiografen.se/). The funders had no role in study design, data collection and analysis, decision to publish, or preparation of the manuscript.

DISCLOSURE

The authors have no commercial or other associations that might constitute a conflict of interest.

REFERENCES

1. Hagberg L, Briles D, Svanborg-Edén C. Evidence for separate genetic defects in C3H/HeJ and C3HeB/FeJ mice that affect the susceptibility to Gram-negative infections.*JImmunol* 1985; **134:** 4118-4122.

2. Frendeus B, Godaly G, Hang L, Karpman D, *et al.*Interleukin 8 receptor deficiency confers susceptibility to acute experimental pyelonephritis and may have a human counterpart. *J Exp Med* 2000; **192:** 881-890.

3. Ragnarsdottir B, Jonsson K, Urbano A, Gronberg-Hernandez J, *et al.*Toll-like receptor 4 promoter polymorphisms: common TLR4 variants may protect against severe urinary tract infection. *PLoS One* 2010; **5:** e10734.

4. Fischer H, Lutay N, Ragnarsdóttir R, Yadav M, *et al.* IRF3-dependent signaling, human polymorphisms and innate resistance to kidney infection. *Plos Pathogen* 2010; **6:** e1001109.

5. Rushton HG. Urinary tract infections in children. Epidemiology, evaluation, and management. *Pediatr Clin North Am* 1997; **44:** 1133-1169.

6. Lin KY, Chiu NT, Chen MJ, Lai CH, *et al.* Acute pyelonephritis and sequelae of renal scar in pediatric first febrile urinary tract infection. *Pediatr Nephrol* 2003; **18:** 362-365.

7. Kunin C. *Detection, prevention and management of urinary tract infections*. Lea and Febiger: Philadelphia, USA, 1987.

8. Mak RH, Kuo HJ. Pathogenesis of urinary tract infection: an update. *Curr Opin Pediatr* 2006; **18:** 148-152.

9. Hang L, Frendeus B, Godaly G, Svanborg C. Interleukin-8 receptor knockout mice have subepithelial neutrophil entrapment and renal scarring following acute pyelonephritis. *J Infect Dis* 2000; **182:** 1738-1748.

10. Lundstedt AC, McCarthy S, Gustafsson MC, Godaly G, *et al.* A genetic basis of susceptibility to acute pyelonephritis. *PLoS One* 2007; **2:** e825.

11. Gehring NH, Frede U, Neu-Yilik G, Hundsdoerfer P, *et al.* Increased efficiency of mRNA 3' end formation: a new genetic mechanism contributing to hereditary thrombophilia. *Nat Genet* 2001; **28:** 389-392.

12. Godaly G, Proudfoot AE, Offord RE, Svanborg C, *et al.*Role of epithelial interleukin-8 (IL-8) and neutrophil IL-8 receptor A in Escherichia coli-induced transuroepithelial neutrophil migration. *Infect Immun* 1997; **65:** 3451-3456.

13. Godaly G, Hang L, Frendeus B, Svanborg C. Transepithelial neutrophil migration is CXCR1 dependent in vitro and is defective in IL-8 receptor knockout mice. *J Immunol* 2000; **165:** 5287-5294.

14. Baggiolini M. Introduction to chemokines and chemokine antagonists. *Ernst Schering Res Found Workshop* 2004**:** 1-9.

15. Fu W, Zhang Y, Zhang J, Chen WF. Cloning and characterization of mouse homolog of the CXC chemokine receptor CXCR1. *Cytokine* 2005; **31:** 9-17.

16. Moepps B, Nuesseler E, Braun M, Gierschik P. A homolog of the human chemokine receptor CXCR1 is expressed in the mouse. *Mol Immunol* 2006; **43:** 897-914.

17. Fan X, Patera AC, Pong-Kennedy A, Deno G, *et al.* Murine CXCR1 is a functional receptor for GCP-2/CXCL6 and interleukin-8/CXCL8. *J Biol Chem* 2007; **282:** 11658-11666.

18. McColl SR, Clark-Lewis I. Inhibition of murine neutrophil recruitment in vivo by CXC chemokine receptor antagonists. *J Immunol* 1999; **163:** 2829-2835.

19. Hang L, Haraoka M, Agace WW, Leffler H, *et al.* Macrophage inflammatory protein-2 is required for neutrophil passage across the epithelial barrier of the infected urinary tract. *J Immunol* 1999; **162:** 3037-3044.

20. Svensson M, Irjala H, Alm P, Holmqvist B, *et al.*Natural history of renal scarring in susceptible mIL-8Rh-/- mice. *Kidney Int* 2005; **67:** 103-110.

21. Dean M, Carrington M, Winkler C, Huttley GA, *et al.* Genetic restriction of HIV-1 infection and progression to AIDS by a deletion allele of the CKR5 structural gene. Hemophilia Growth and Development Study, Multicenter AIDS Cohort Study, Multicenter Hemophilia Cohort Study, San Francisco City Cohort, ALIVE Study. *Science* 1996; **273:** 1856-1862.

22. Liu R, Paxton WA, Choe S, Ceradini D, *et al.* Homozygous defect in HIV-1 coreceptor accounts for resistance of some multiply-exposed individuals to HIV-1 infection. *Cell* 1996; **86:** 367-377.

23. Samson M, Libert F, Doranz BJ, Rucker J, *et al.* Resistance to HIV-1 infection in caucasian individuals bearing mutant alleles of the CCR-5 chemokine receptor gene. *Nature* 1996; **382:** 722-725.

24. Vasilescu A, Terashima Y, Enomoto M, Heath S, *et al.* A haplotype of the human CXCR1 gene protective against rapid disease progression in HIV-1+ patients. *Proc Natl Acad Sci U S A* 2007; **104:** 3354-3359.

25. Wagenlehner FM, Pilatz A, Naber KG, Weidner W. Therapeutic challenges of urosepsis. *Eur J Clin Invest* 2008; **38 Suppl 2:** 45-49.

26. Sutherland AM, Walley KR. Bench-to-bedside review: Association of genetic variation with sepsis. *Crit Care* 2009; **13:** 210.

27. Agace W, Hedges S, Ceska M, Svanborg C. IL-8 and the neutrophil response to mucosal Gram negative infection. *J Clin Invest* 1993; **92:** 780-785.

28. Hedges S, Agace W, Svanborg C. Epithelial cytokine responses and mucosal cytokine networks. *Trends in Microbiol* 1995; **3:** 266-270.

29. Otto G, Burdick M, Strieter R, Godaly G. Chemokine response to febrile urinary tract infection. *Kidney Int* 2005; **68:** 62-70.

30. Godaly G, Bergsten G, Hang L, Fischer H, *et al.* Neutrophil recruitment, chemokine receptors, and resistance to mucosal infection. *J Leukoc Biol* 2001; **69:** 899-906.

31. Chowdhury P, Sacks SH, Sheerin NS. Minireview: functions of the renal tract epithelium in coordinating the innate immune response to infection. *Kidney Int* 2004; **66:** 1334-1344.

32. Xia Y, Feng L, Yoshimura T, Wilson CB. LPS-induced MCP-1, IL-1 beta, and TNF-alpha mRNA expression in isolated erythrocyte-perfused rat kidney. *Am J Physiol* 1993; **264:** F774-780.

33. Schlondorff D, Nelson PJ, Luckow B, Banas B. Chemokines and renal disease. *Kidney Int* 1997; **51:** 610-621.

34. Ascon M, Ascon DB, Liu M, Cheadle C, *et al.* Renal ischemia-reperfusion leads to long term infiltration of activated and effector-memory T lymphocytes. *Kidney Int* 2009; **75:** 526-535.

35. Majno G, Joris I. Apoptosis, oncosis, and necrosis. An overview of cell death. *Am J Pathol* 1995; **146:** 3-15.

36. Saville J, Dransfield I, Hogg N, Haslett C. Vitronectine receptor-mediated phagocytosis of cells undergoing apoptosis. *Nature* 1990; **343:** 170-173.

37. Levine J, Neitlich J, Smith RC. The value of prone scanning to distinguish ureterovesical junction stones from ureteral stones that have passed into the bladder: leave no stone unturned. *AJR Am J Roentgenol* 1999; **172:** 977-981.

38. Duffield JS, Bonventre JV. Kidney tubular epithelium is restored without replacement with bone marrow-derived cells during repair after ischemic injury. *Kidney Int* 2005; **68:** 1956-1961.

39. Lin F, Moran A, Igarashi P. Intrarenal cells, not bone marrow-derived cells, are the major source for regeneration in postischemic kidney. *J Clin Invest* 2005; **115:** 1756-1764.

40. Mårild S, Jodal U, Ørskov I, Ørskov F, *et al.* Special virulence of the *Escherichia coli* O1:K1:H7 clone in acute pyelonephritis. *J Pediatr* 1989; **115:** 40-45.

41. Connell H, Wilson I, Sabharwal H, Persson L, *et al.* Determinants of *Escherichia coli* growth in human urine. *Chemotherapy* 1996; **In Press**.

42. Cacalano G, Le J, Kikly K, Ryan AM, *et al.* Neutrophil and B cell expansion in mice that lack the murine IL-8 receptor homolog. *Science* 1994; **265:** 682-684.

43. Hagberg L, Hull R, Hull S, Falkow S, *et al.* Contribution of adhesion to bacterial persistence in the mouse urinary tract. *Infect Immun* 1983; **40:** 265-272.

FIGURE LEGENDS

Figure 1. *mCxcr2*genotyping and *mCxcr2* expression of *mCxcr2*$^{+/+}$, *mCxcr2*$^{+/-}$ and *mCxcr2*$^{-/-}$ mice. (A) *mCxcr2* genotype as determined by polymerase chain reaction (PCR) using primers specific for *mCXCR2* for the neomycin gene. (B) Neutrophil mCXCR2 surface expression in *mCxcr2*$^{+/+}$, *mCxcr2*$^{+/-}$ and *mCxcr2*$^{-/-}$ mice, quantified by flow cytometry. *mCxcr2*$^{-/-}$ mice (white) had no receptor expression, as verified by comparison with the IgG isotype control, *mCxcr2*$^{+/-}$ (grey) and *mCxcr2*$^{+/+}$ (black). (C) Relative mCXCR2 mRNA expression (compared to GAPDH). Results are means ± SEM (**p < 0.01, ***p ≤ 0.001). Representative data are shown from five separate experiments.

Figure 2. Sepsis-related mortality, bacterial counts and kidney morphology in *mCxcr2*$^{+/+}$, *mCxcr2*$^{+/-}$ and *mCxcr2*$^{-/-}$ mice. (A) Kaplan-Meier survival curve after intravesical infection of *mCxcr2*$^{+/+}$, *mCxcr2*$^{+/-}$ and *mCxcr2*$^{-/-}$ mice (p<0.001, *mCxcr2*$^{+/+}$ versus *mCxcr2*$^{-/+}$; p<0.001 heterozygous versus homozygous). (B) Bacterial counts in the kidneys of *mCxcr2*$^{+/+}$ and *mCxcr2*$^{+/-}$ mice (ns = not significant). (C) Kidney morphology of *mCxcr2*$^{+/+}$, *mCxcr2*$^{+/-}$ and *mCxcr2*$^{-/-}$ mice, 28 days after infection.

Figure 3. Differences in neutrophil and cytokine responses to infection between *mCxcr2*$^{+/+}$and *mCxcr2* $^{+/-}$mice. (A) Secretion of mCXCL2/3 and (B) mCCL2 into urine after infection of *mCxcr2*$^{+/+}$ and *mCxcr2*$^{+/-}$ mice with *E. coli* 1177. (C) Neutrophil counts in urine of *mCxcr2*$^{+/+}$ and *mCxcr2* $^{+/-}$mice. Samples were obtained before infection (0 h) and 2, 6, and 24 hours and from 7 days to 42 days after inoculation. Results are means ± SEM (*p < 0.05, **p < 0.01, 8–10 mice/time point).

Figure 4. Neutrophil response, epithelial damage and neutrophil accumulation in the kidneys of infected *mCxcr2*$^{+/+}$ and *mCxcr2*$^{+/-}$ mice.

(A) Early sub-epithelial neutrophil influx in wild type mice after 6 hours of infection. Wild type mice show intact epithelium and no neutrophil accumulation.

(B) Delayed sub-epithelial neutrophil influx (arrows) and neutrophil accumulation (*) 7 days after infection in heterozygous mice. Proliferating epithelium was observed 14 days after infection in *mCxcr2*$^{+/-}$ mice.

Haematoxylin-eosin staining (left panel) and immunohistochemistry, using the monoclonal granulocyte-specific antibody (RB6-8C5)(right panel).

Figure 5. Epithelial hypertrophy and tissue fibrosis in *mCxcr2*$^{+/+}$, *mCxcr2*$^{+/-}$ and *mCxcr2*$^{-/-}$ mice.

(A) Minor epithelial proliferation in *mCxcr2*$^{+/+}$ mice, 7 days after infection, but no evidence of fibrosis.

(B) In *mCxcr2*$^{+/-}$mice sub-epithelial fibrosis and epithelial hypertrophywas observed 7 days after infection. Proliferating epithelium was seen after 14 days of infection in the *mCxcr2*$^{+/-}$ mice.

(C) Thickening of the pelvic epithelium and fibrosis were observed 7 days post-infection in the *mCxcr2*$^{-/-}$ mice. After twenty-eight days the inflammatory cell infiltrate was abundant and Russel bodies were observed. Thirty-five days post-infection the tissue was destroyed and replaced by abscesses and inflammatory cells.

Proliferation is visualised by hematoxylin-eosin staining and Masson's trichrome was used to visualise tissue fibrosis (blue).

Figure 6. Overview of the disease in *mCxcr2*$^{+/-}$ mice

A collected overview of the course of disease in *mCxcr2*$^{+/-}$ mice, showing neutrophil accumulation in the lumen (RB6-8C5and DAPI), and epithelial proliferation and fibrosis as indicated by arrows (L=lumen, E=epithelium).

SUPPLEMENTARY FIGURE LEGEND

Figure S1. Macrophage recruitment into the kidneys of *mCxcr2*$^{+/+}$ and *mCxcr2*$^{+/-}$ mice.

Macrophage staining was not observed in the *mCxcr2*$^{+/+}$ mice at 7 - 48 days after infection. In *mCxcr2*$^{+/-}$ mice, macrophages were observed in the medulla and cortex in 10% of the mice on day 42 after infection, but not after 35 days (right panel). Haematoxylin-eosin staining (middle) and Immunohistochemistry (right panel),

Figure 1

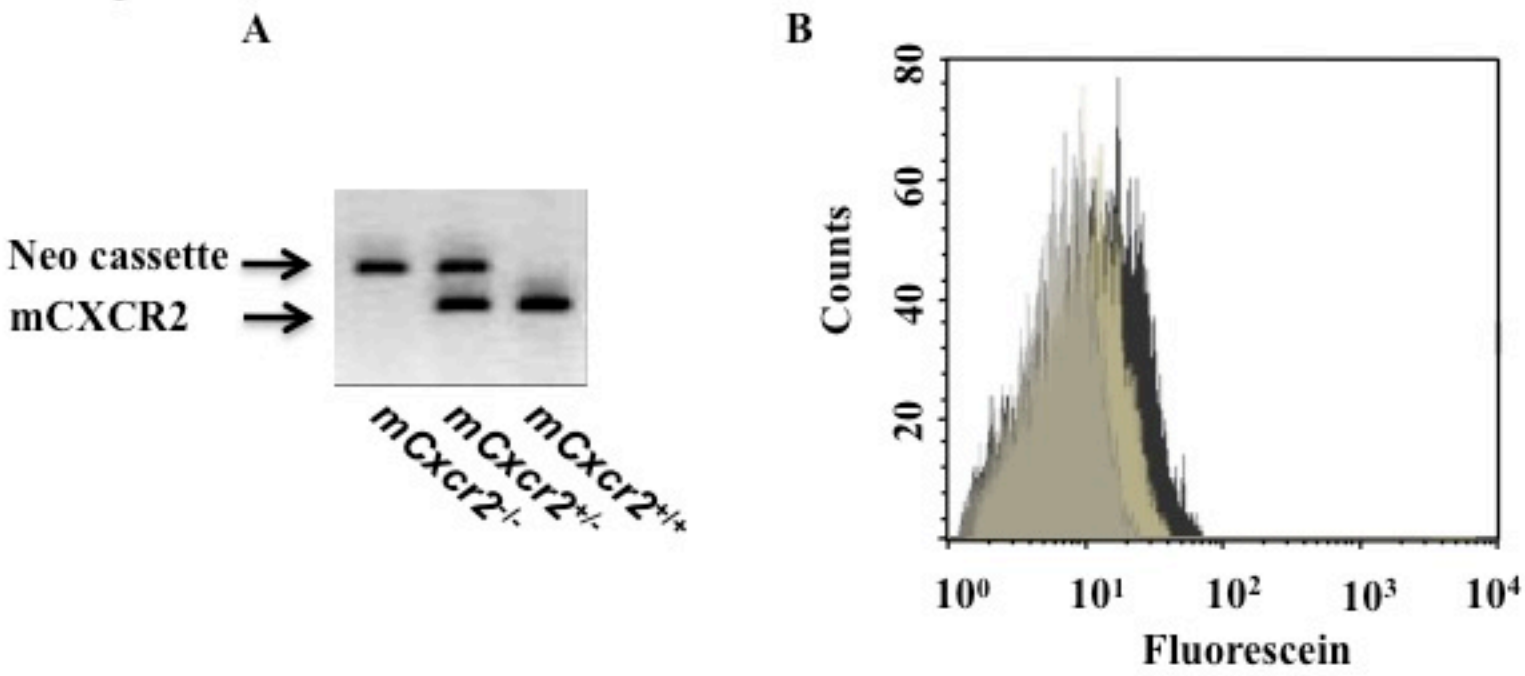
A
Neo cassette
mCXCR2
mCxcr2-/-
mCxcr2+/-
mCxcr2+/+
B
Counts
80
60
40
20
10⁰
10¹
10²
10³
10⁴
Fluorescein
C
CXCR2/GAPDH
0.045
0.035
0.025
0.015
0.005
**
***
***
mCxcr2+/+
mCxcr2+/-
mCxcr2-/-

Figure 2

A

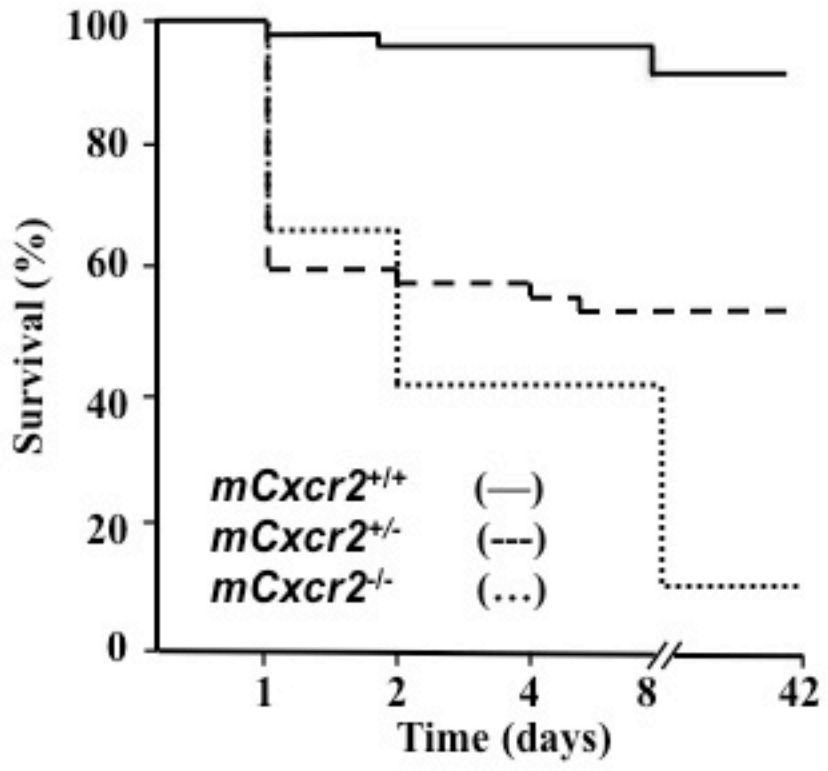

B

Time post infection (days)	*mCxcr2*$^{+/+}$mice CFU/mL (± SEM)	*mCxcr2*$^{+/-}$mice CFU/mL (± SEM)	P values
0.4	$24x10^5 \pm 11x10^3$	$3x10^3 \pm 2x10^4$	ns
7	18 ± 17	$53x10^3 \pm 3x10^3$	0.01
14	2 ± 3	$53x10^3 \pm 4x10^3$	0.01
21	2 ± 1	11 ± 2	0.01
28	1 ± 0	1 ± 0	ns
42	1 ± 0	1 ± 0	ns

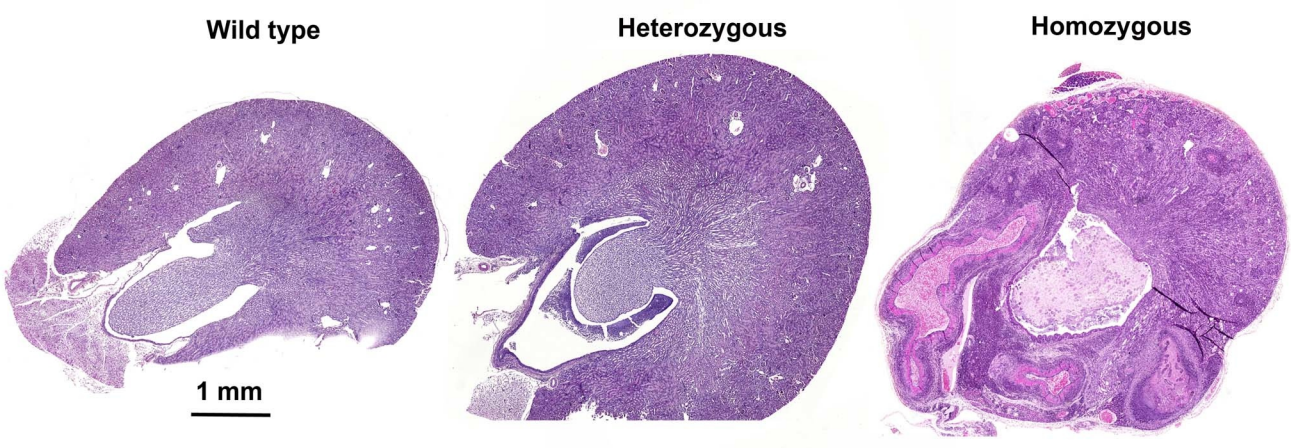
Wild type
Heterozygous
Homozygous
1 mm

Figure 3

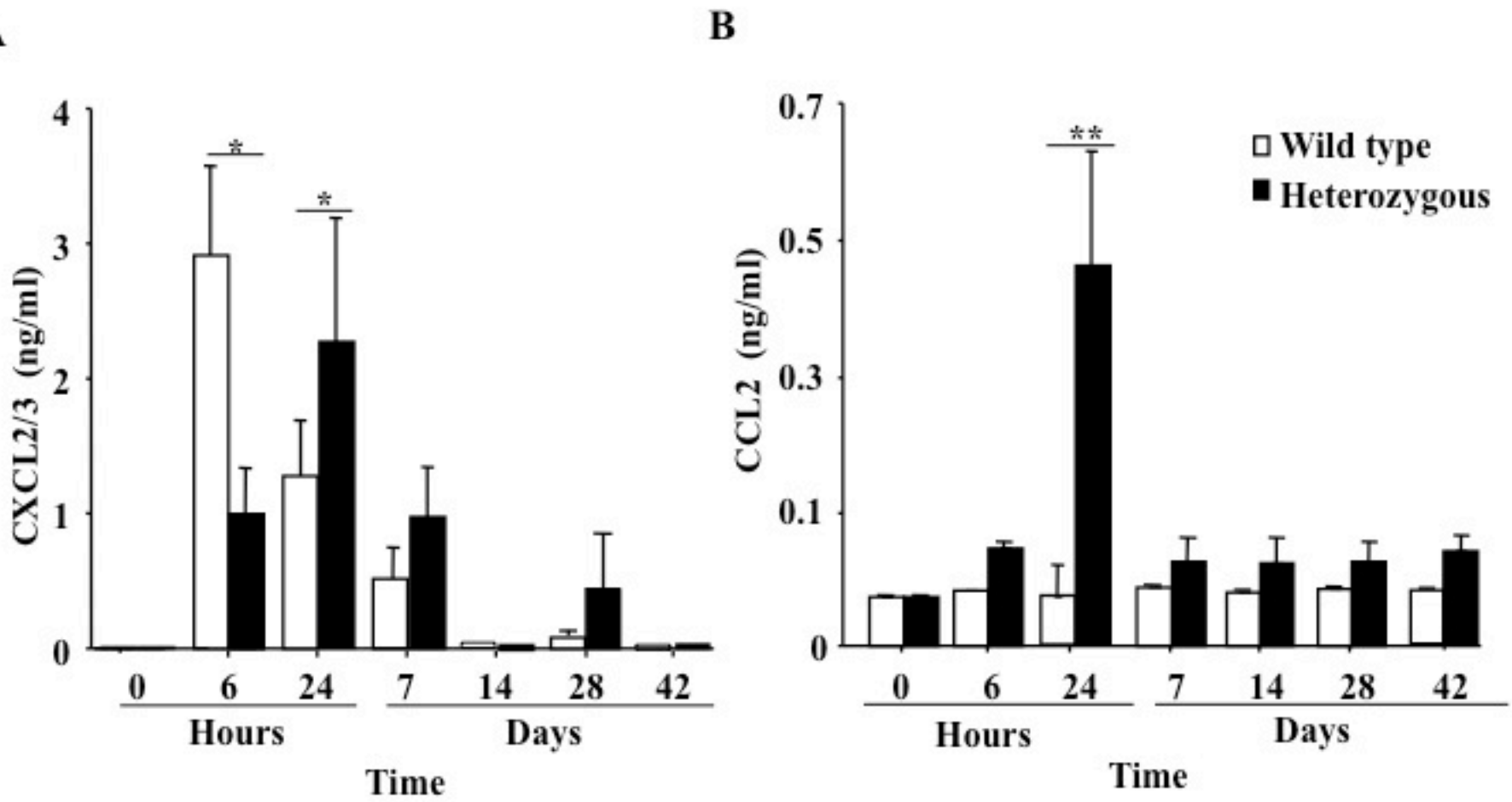
A
CXCL2/3 (ng/ml)
4
3
2
1
0
*
*
0
6
24
7
14
28
42
Hours
Days
Time
B
CCL2 (ng/ml)
0.7
0.5
0.3
0.1
0
**
Wild type
Heterozygous
0
6
24
7
14
28
42
Hours
Days
Time

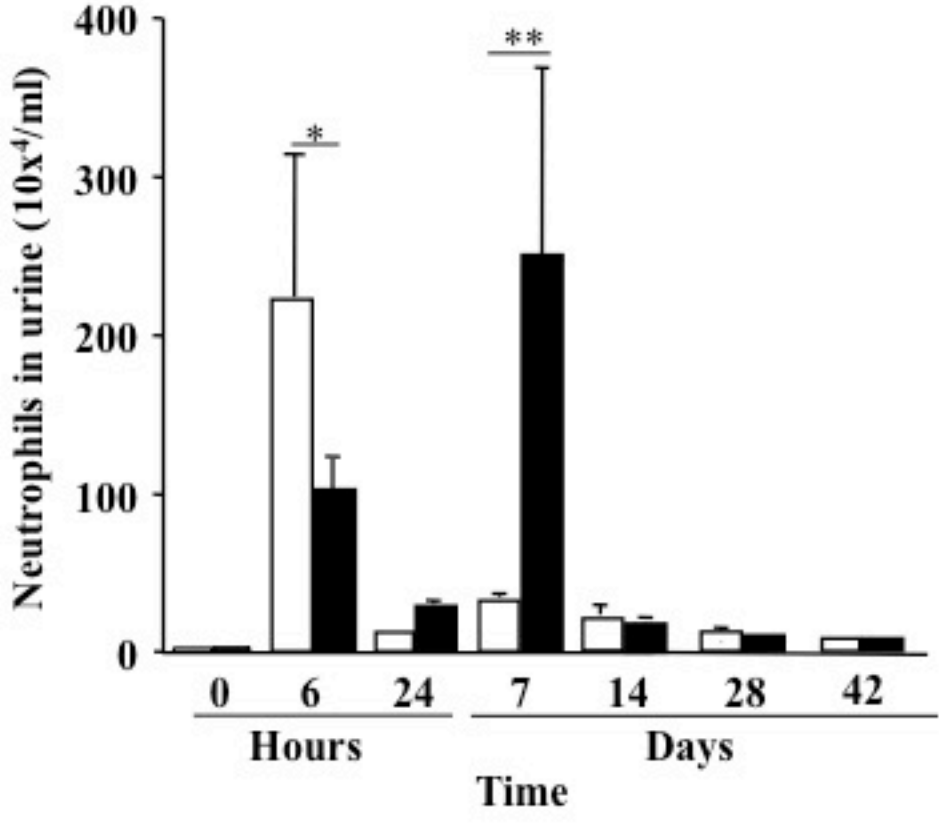
C
Neutrophils in urine (10x4/ml)
400
300
200
100
0
*
**
0
6
24
7
14
28
42
Hours
Days
Time

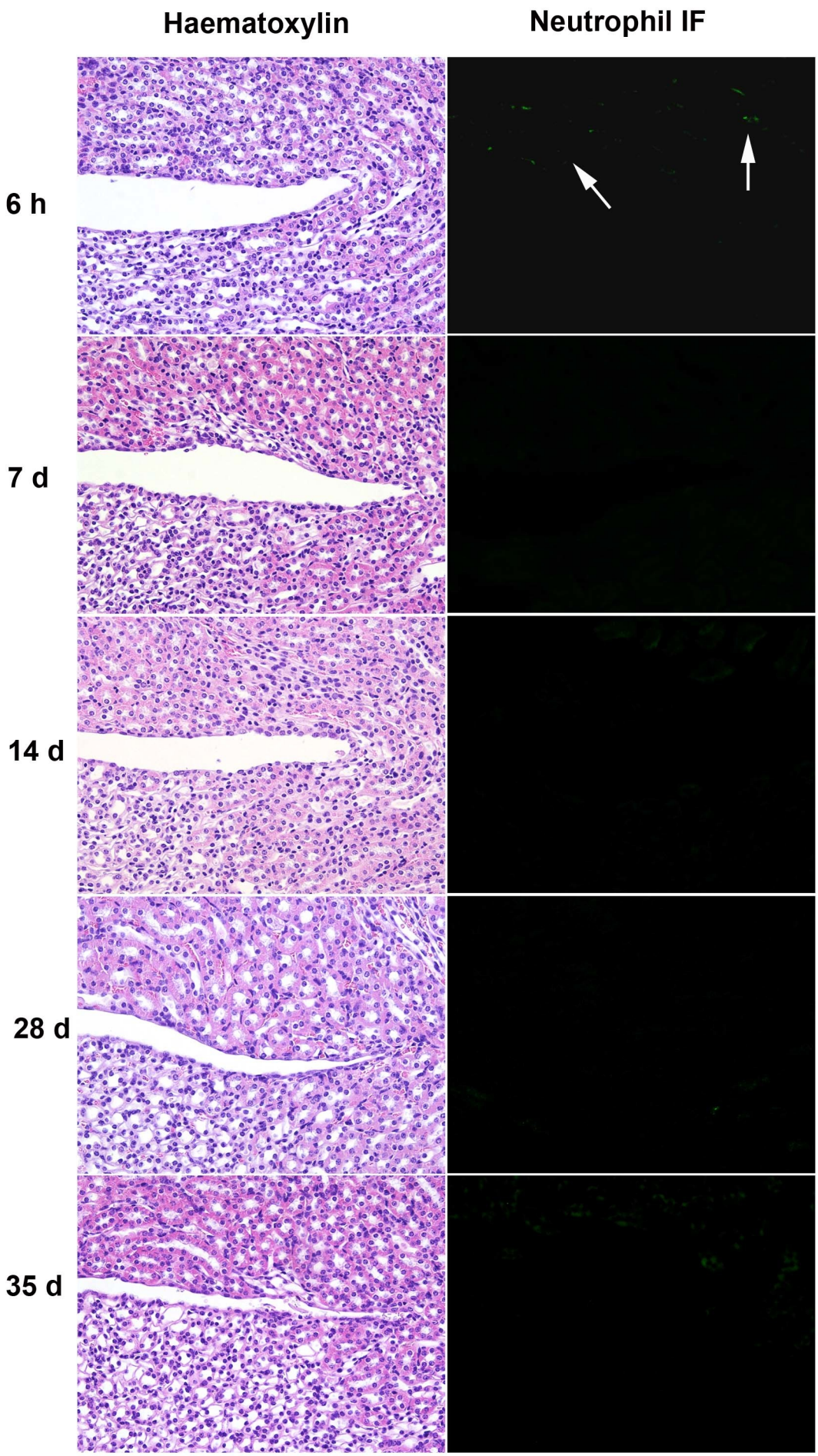
Haematoxylin
Neutrophil IF
6 h
7 d
14 d
28 d
35 d

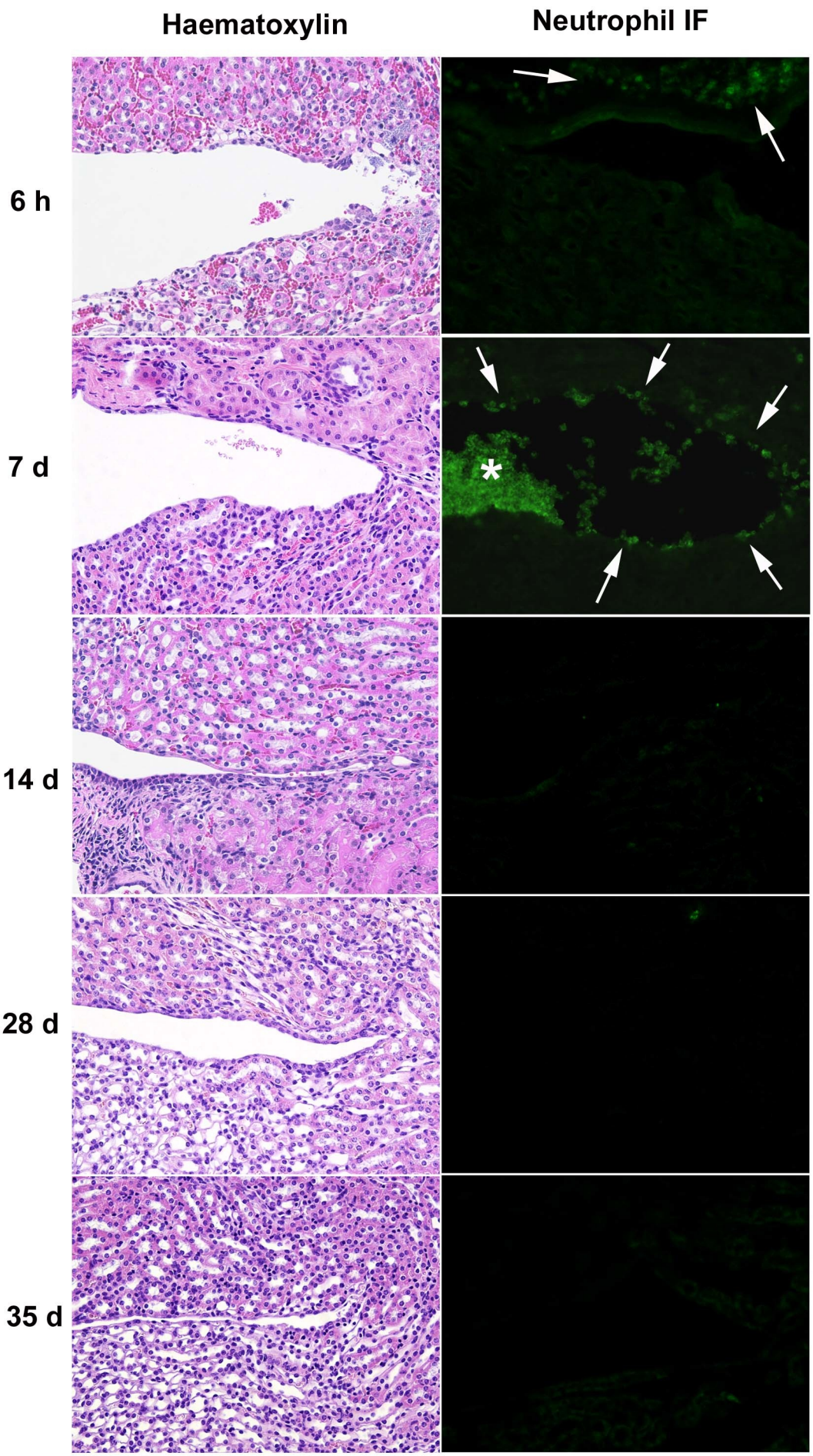
Haematoxylin
Neutrophil IF
6 h
7 d
14 d
28 d
35 d
*

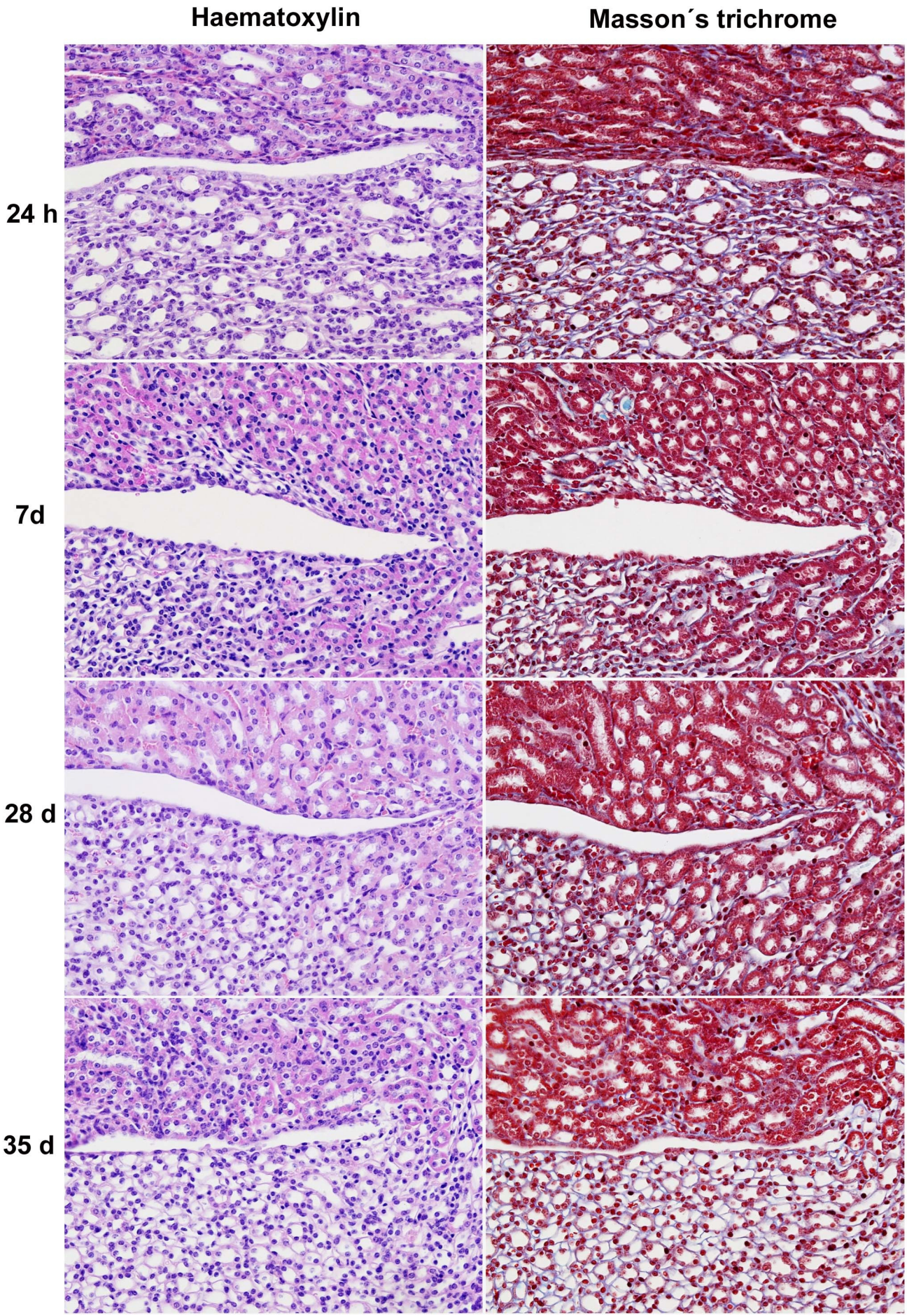
Haematoxylin
Masson´s trichrome
24 h
7d
28 d
35 d

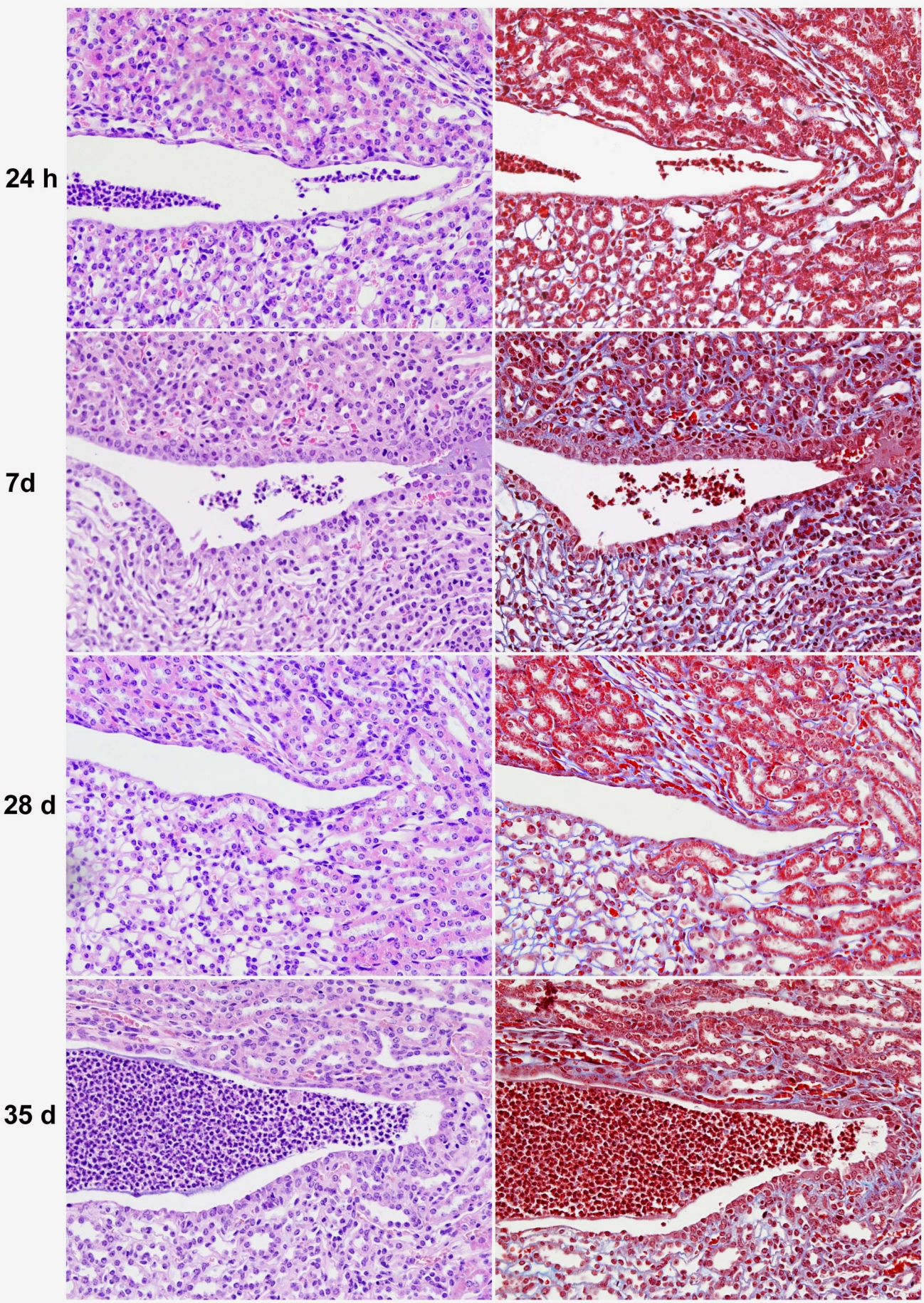
Haematoxylin
Masson´s trichrome
24 h
7d
28 d
35 d

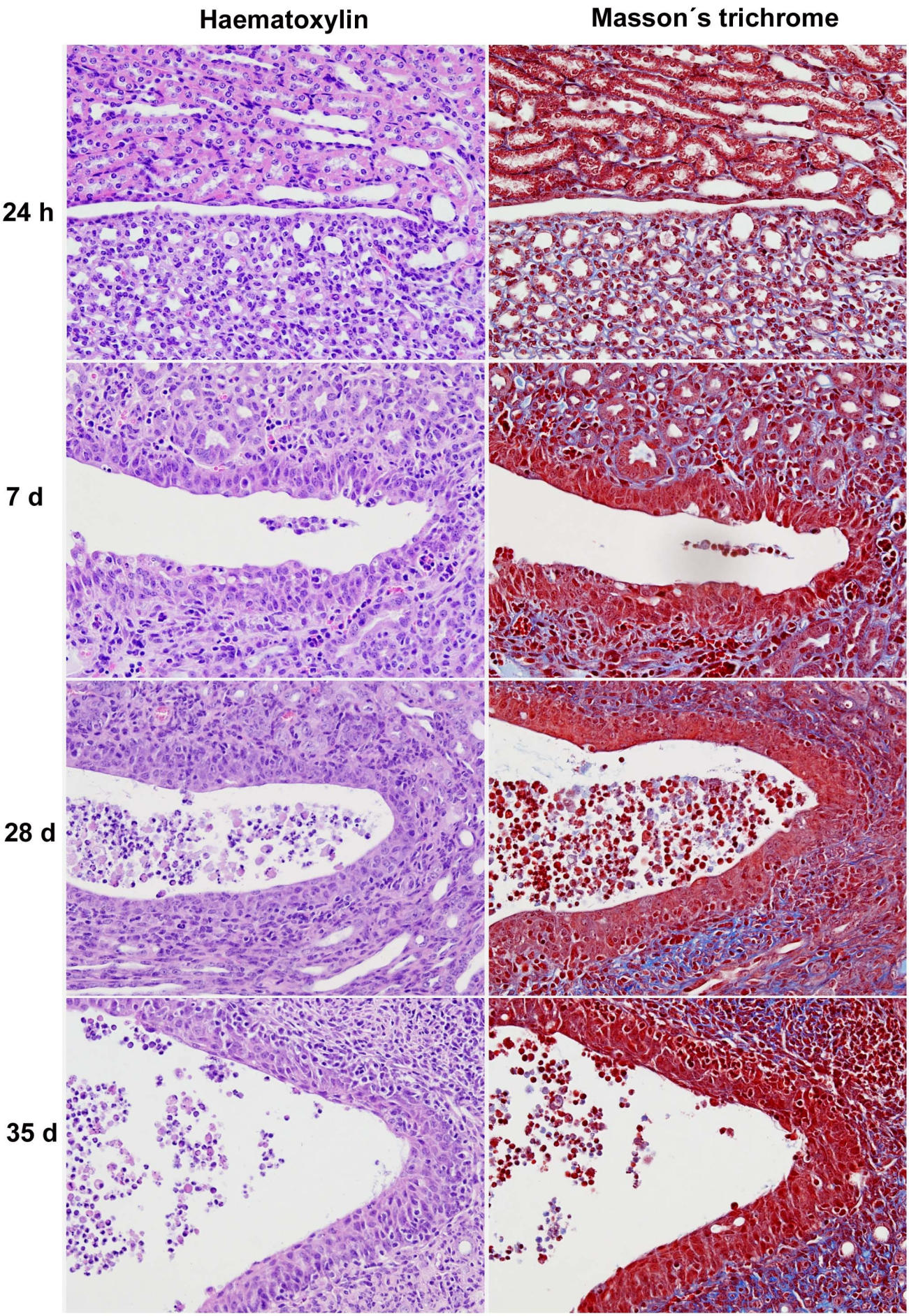
Haematoxylin
Masson´s trichrome
24 h
7 d
28 d
35 d

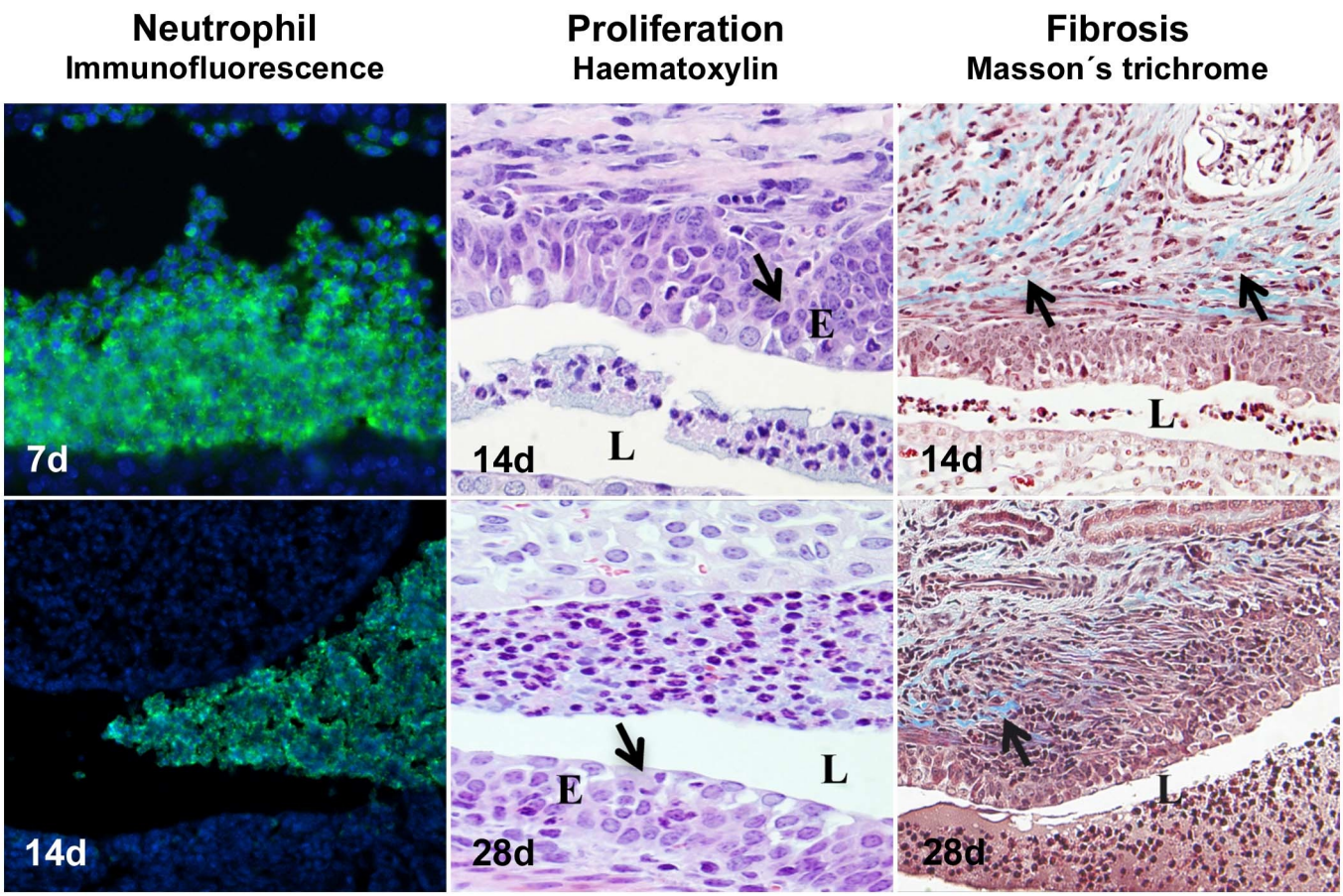
Neutrophil
Immunofluorescence
Proliferation
Haematoxylin
Fibrosis
Masson´s trichrome
7d
14d
L
E
14d
L
14d
28d
E
L
28d
L